THE ASTROPHYSICAL JOURNAL, 465:650–658, 1996 July 10

THE PROPERTIES OF X-RAY SELECTED ACTIVE GALACTIC NUCLEI. IV. THE LOCAL OPTICAL LUMINOSITY FUNCTION OF BROAD-LINE ACTIVE GALACTIC NUCLEI

ROBERTO DELLA CECA,[1] GIOVANNI ZAMORANI,[2,3] TOMMASO MACCACARO,[4]
GIANCARLO SETTI,[3,5] AND ANNA WOLTER[4]
Received 1995 March 2; accepted 1996 January 22

ABSTRACT

We have selected a local ($z \leq 0.3$) subsample of 226 broad line active galactic nuclei (BLAGNs) from the *Einstein Observatory* Extended Medium Sensitivity Survey. This sample represents the largest unbiased and complete sample of local BLAGNs ever assembled and has allowed us to derive their space density in regions of the $m_B - z$ plane where, with the usual optical selection criteria, it is very difficult to obtain complete samples of BLAGNs.

Using total integrated magnitudes (i.e., nucleus + host galaxy), we have computed the *local* optical luminosity function of this X-ray selected sample and compared it with those derived from local optical samples. Thanks to the large number of objects at our disposal we can set more stringent constraints on the space density of BLAGNs than has previously been possible. The luminosity function derived from our sample is in good agreement with the composite luminosity function which can be derived from optically selected samples only by using different selection criteria in different ranges of absolute magnitude. In particular, at low luminosity ($M_B \geq -22$) we confirm the flattening of the local optical luminosity function originally suggested by Meurs & Wilson (1984) while in the magnitude range from $M_B \sim -23$ to -25 we find a very good agreement with the optical spatial density derived using data from the Bright Quasars Survey.

By convolving our luminosity function with the distribution of the ratio of nuclear to total flux of a sample of $\sim$40 Seyfert 1 and 1.5 galaxies from the literature, we have also derived an estimate for the *nuclear* luminosity function of BLAGNs. This nuclear luminosity function is in rather good agreement with the nuclear luminosity functions previously derived, using a much smaller number of objects, from optical samples of low-luminosity BLAGNs. A reasonably good agreement is also found between our luminosity function and the extrapolation to low redshift ($z = 0.15$, the average redshift of our sample) of the quasar luminosity function derived from more than 1000 optically selected quasars. The integration of our nuclear luminosity function over the $M_B - z$ plane shows that good agreement is obtained with the observed number counts of low luminosity ($M_B \geq -23$) BLAGNs at faint magnitudes, if the $M_B \geq -23$ population evolves similarly to the QSO population.

Subject headings: galaxies: active — galaxies: evolution — galaxies: luminosity function, mass function — galaxies: nuclei

1. INTRODUCTION

A good knowledge of the *local* spatial density of extragalactic objects is essential for studies of their evolutionary properties. In the case of the broad-line active galactic nuclei (BLAGNs)[6] the determination of their local spatial density allows us, for example, to verify if they are the local counterparts of the more distant QSOs (Cavaliere, Giallongo, & Vagnetti 1985), to evaluate the fraction of "normal galaxies" that harbor AGNs (Cavaliere & Padovani 1988, 1989), to study their role in the process of the galaxy formation (Haehnelt & Rees 1993), to compute their contribution to the X-ray (Comastri et al. 1995; Madau, Ghisellini, & Fabian 1994) and UV backgrounds (Madau 1992), and to test the unification models recently proposed to explain their overall properties (see the review of Antonucci 1993)

Many authors have studied the optical luminosity function of broad-line Seyfert galaxies (e.g., Meurs & Wilson 1984, hereafter MW84; Marshall 1987, hereafter M87; Huchra & Burg 1992, hereafter HB92). Unfortunately, optical samples of low-luminosity AGNs ($M_B \gtrsim -23$) can suffer from major selection effects and/or incompleteness that can seriously limit their usefulness. For example, the classical ultraviolet-excess surveys (e.g., the Markarian survey; Markarian & Lipovetskii 1976, and references therein) are well known to be biased against low-luminosity AGNs because of the significant flux contribution from the host galaxy.

Because of these selection effects it is very difficult to define and select, with a single selection criterion, a *complete* flux-limited sample of Seyfert galaxies. One possible solution is to select a sample of BLAGNs from a complete spectroscopic sample of galaxies. This method was used by HB92 to compute the optical luminosity function of Seyfert

[1] Department of Physics and Astronomy, Johns Hopkins University, Homewood Campus, Baltimore, MD 21218.
[2] Osservatorio Astronomico di Bologna, via Zamboni 33, 40126 Bologna, Italy.
[3] Istituto di Radioastronomia del CNR, via Gobetti 101, 40129 Bologna, Italy.
[4] Osservatorio Astronomico di Brera, via Brera 28, 20121 Milano, Italy.
[5] Dipartimento di Astronomia, via Zamboni 33, 40126 Bologna, Italy.
[6] For the purpose of this paper we use the term BLAGNs to refer to those objects showing broad (FWHM $\geq$ 1000 km s^{-1}) emission lines and evidence of a nonstellar continuum, regardless of their appearance on the Palomar Observatory Sky Survey and of their absolute magnitude (i.e., Seyfert 2 galaxies, BL Lacertae objects, and LINERs are excluded).

1 and Seyfert 2 galaxies, starting from the 26 Seyfert 1 galaxies and the 23 Seyfert 2 galaxies discovered in the CfA redshift survey.[7] However, this approach needs a large amount of optical telescope time because only a fraction between ~1% (HB92) and ~10% (Ho, Filippenko, & Sargent 1995) of the field galaxies at any given apparent magnitude may host a BLAGN. Furthermore, this approach may result in significant incompleteness when the nuclei are very bright. In this case the object may appear stellar and may not be included in the list of galaxies to be investigated for activity.

Since soft X-ray emission is a fundamental property of BLAGNs (Avni & Tananbaum 1986; Wilkes et al. 1994), sizable samples of these objects can be constructed through optical identification of soft X-ray sources and these samples of objects are *independent* of their optical appearance.

In a recent paper, Franceschini et al. (1994) have addressed the problem of the comparison between the luminosity functions and the evolution rates of X-ray selected and optically selected AGNs. In particular, these authors have discussed the "quasar side" ($M_B \lesssim -23$) of the $z - M_B$ distribution and they conclude that optical and soft X-ray observations appear to detect the same population of objects.

In this paper we consider instead the objects on the low-luminosity and low-redshift side of the $z - M_B$ distribution. Are the X-ray and optical selection techniques sampling the same types of objects also in this luminosity interval? In particular, are the spatial densities found with the two selection techniques comparable?

We have been prompted by these questions to derive the local (i.e., $z \leq 0.3$) optical luminosity function of X-ray selected BLAGNs and to compare it with the luminosity functions obtained from the optical samples. Because of the large number of objects at our disposal, we should be able to better constrain the local spatial density of BLAGNs and, in particular, of low-luminosity ($M_B \geq -23$) BLAGNs.

The completion of the *Einstein Observatory* Extended Medium Sensitivity Survey (EMSS) (Gioia et al. 1990; Stocke et al. 1991; Maccacaro et al. 1994) and the almost complete identification rate (~97.5%) allows us to extract a subsample of BLAGNs suitable for statistical studies (see Maccacaro et al. 1994 for an update of the optical identifications of the EMSS sample). The sample used in the present paper consists of 226 objects and represents the largest unbiased sample of local broad-line Seyfert galaxies ever assembled. The paper is organized as follows: the sample used is described in § 2, where a brief discussion is also given of the corrections applied to the original EMSS sample in order to deal with the contamination of narrow-line AGNs; in § 3 we derive the local optical luminosity function of X-ray selected BLAGNs and compare it with the optical luminosity function of BLAGNs derived from optical samples. In § 4, we derive an estimate of the *nuclear* luminosity function of BLAGNs. In § 5 we integrate this nuclear luminosity function over the $M_B - z$ plane to estimate the number counts of broad-line low-luminosity ($M_B \geq -23$) AGNs at faint magnitudes; we compare this prediction with the number density found in optically selected samples. Finally, in § 6 we summarize and discuss the results obtained.

Throughout the paper a Hubble constant of 50 km s^{-1} Mpc^{-1} and a Friedmann universe with a deceleration parameter $q_0 = 0$ are assumed.

2. THE DATA

The EMSS contains 437 spectroscopically identified X-ray selected AGNs (Maccacaro et al. 1994, and references therein); their distribution in the $z - M_B$ plane is shown in Figure 1. In order to derive the *local* optical luminosity function, we have considered in this paper only the 243 X-ray selected AGNs with $z \leq 0.3$. As discussed in § 3, cosmological evolution effects do not appear to be significant for our sample within the chosen redshift range. It is worth noting that in this redshift range we are principally sampling objects on the low-luminosity side of the $z - M_B$ distribution with just a few objects brighter than $M_B = -24$.

The EMSS sample of AGNs also contains some narrow-line objects (e.g., Seyfert 2, low-ionization nuclear emission-line region [LINER], starburst galaxies). For the purposes of this paper these objects should be considered as a contamination of the population of BLAGNs. These "possible" narrow-line objects are listed in Table 8 and 10 of Stocke et al. (1991) (31 AGNs in total with $z \leq 0.3$). However, many of these objects were included in these tables simply because the S/N in their spectra was insufficient to ascertain if a broad-line component was present. New spectroscopic data at higher resolution are now available for many of these objects (Griffiths et al. 1996 and references therein). Of the 31 AGNs with $z \leq 0.3$ originally listed in Table 8 and 10 of Stocke et al. (1991), 10 are now confirmed BLAGNs, 12 are confirmed narrow-line objects (Seyfert 2 or starburst galaxies), eight remain "possible" narrow-line objects, and one object (MS 1532.5+0130) has been now reclassified as a cluster of galaxies. After removing from the sample the 12

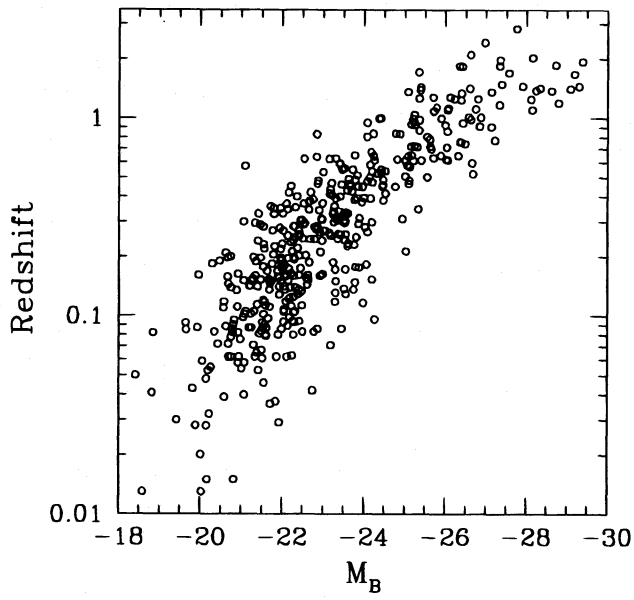

FIG. 1.—Distribution of the complete EMSS AGNs sample (437 objects) in the $M_B - z$ plane.

[7] The Center for Astrophysics (CfA) Redshift survey (Davis, Huchra, & Latham 1983; Huchra et al. 1983) covers ≃2.7 sr of sky to a magnitude limit of $B_{tot} = 14.5$. Almost all the ~2400 galaxies in the photometric catalog were spectroscopically investigated and classified for activity on the basis of emission lines in the 4600–7000 Å region.

TABLE 1

EMSS AGN WITH $z \leq 0.3$ EXCLUDED FROM THE ANALYSIS

MS 0340.3+0455	MS 0423.8−1247
MS 1047.3+3518	MS 1058.8+1003
MS 1252.4−0457	MS 1412.8+1320
MS 1414.8−1247	MS 1451.5+2139
MS 1555.1+4522	MS 1614.1+3239
MS 2338.9−1206	MS 2348.6+1956

confirmed narrow-line objects (see Table 1), we are left with a complete flux-limited sample of 231 soft X-ray selected BLAGNs. As will be discussed in § 3, the inclusion in the BLAGNs sample of the eight objects with poor S/N spectra does not have any significant effect on the derived spatial densities.

The X-ray fluxes in the 0.3–3.5 keV energy band are taken from Gioia et al. (1990). Fluxes are computed assuming a power-law spectrum with energy index $\alpha_X = 1$ (see Maccacaro et al. 1988) and have been corrected for absorption using the measured Galactic hydrogen column density along the line of sight to each source (as determined from the H I radio maps; see Gioia et al. 1990 and references therein). Redshifts, V magnitudes, and Galactic N_H values are taken from Stocke et al. (1991) and from Maccacaro et al. (1994). The optical V-band magnitudes come either from CCD photometry (180 objects) or from estimates from the sky survey plates or from the literature. Magnitudes from the literature or from the sky survey plates are all assumed to be accurate to ± 0.5 mag. Where CCD photometry is available, the typical accuracy is 0.05 mag. The CCD magnitudes are determined within a 10″ aperture, corresponding to ~ 25 kpc at $z = 0.1$. In all cases our magnitude estimates should be considered as total magnitudes (i.e., nucleus + host galaxy). We have converted the V magnitudes into B magnitudes assuming $m_B - m_V = 0.8$ if starlight absorption was present (the 24 objects with evidence of H and K Ca absorption in the spectra; see column [13] in Table 4 of Stocke et al. 1991) or $m_B - m_V = 0.3$ if it was not. The magnitude of each object was also corrected for absorption along the line of sight through our Galaxy using the formula for reddening given by Burstein & Heiles (1978), $F_{B-V} = \max[0; \quad -0.055 + 1.987 \times 10^{-22} N_H]$, which assumes a constant gas-to-dust ratio. We have used the extinction in the B band ($A_B = 4.2 \times E_{B-V}$) reported in Hartwick & Shade (1990). The absolute B magnitude was calculated following the procedure given in Schmidt & Green (1983):

$$M_B = m_B - 5 \log (z + 0.5z^2) + 2.5(1 - \alpha) - 43.89$$

by assuming a power-law spectrum ($f_\nu \propto \nu^{-\alpha}$) with $\alpha = 1.0$. No correction has been made for emission lines, broad absorption lines, or other deviations from pure power-law behavior. All these assumptions and corrections produce absolute B magnitudes with an accuracy of about (0.3–0.7) mag.

In Figure 2 we show the distribution in the $m_B - z$ plane; we sample the low-luminosity BLAGNs down to B magnitudes of about of 19–20, i.e., in regions of the $m_B - z$ plane where the usual optical selection methods have difficulties in yielding *complete* flux-limited samples of these objects.

The EMSS sample still suffers from a small incompleteness (24 sources out of 835 have not been identified). Among these unidentified sources only $\sim$five objects are expected

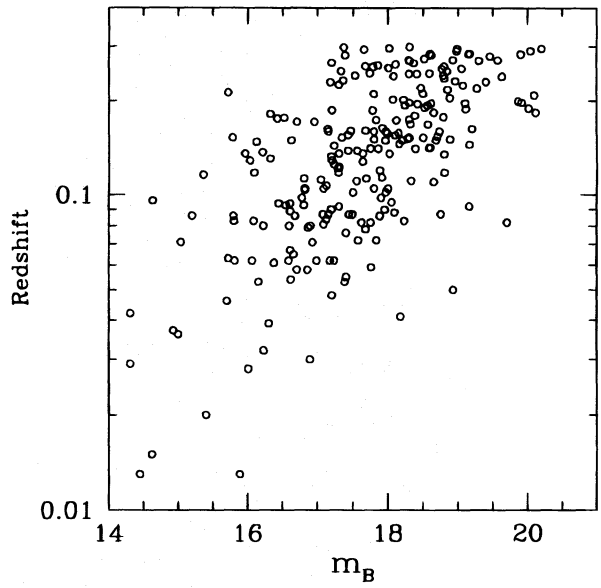

FIG. 2.—Distribution of the X-ray selected BLAGNs with $z \leq 0.3$ in the $m_B - z$ plane.

to be AGNs with $z \leq 0.3$ (see Maccacaro et al. 1991 for details). These sources are very faint in X-rays and, given the relationship between the X-ray and the optical luminosity, are very faint in the optical as well. For all of them there is no plausible optical counterpart visible on the sky survey plates ($m_{\rm lim} \sim 20.5$) within or adjacent to the X-ray error circle. As reported in Stocke et al. (1991), a few of these sources have optical counterparts fainter than the limits of the POSS. In order to take into account this small incompleteness we have used a limiting magnitude, $m_{B_{\rm lim}} = 20$, for the derivation of the optical luminosity function described in the next section. With this choice the BLAGNs sample reduces to 226 X-ray selected AGNs.

3. THE LOCAL OPTICAL LUMINOSITY FUNCTION OF BLAGNs

A nonparametric representation of the observed optical luminosity function in any redshift shell for an optically selected sample can be obtained using the $1/V_a$ method of Avni & Bahcall (1980), which is a generalization of the $1/V_{\rm max}$ method (Schmidt 1968) when several samples are analyzed. Here we apply this method to derive the optical luminosity function in the redshift shell (0.0–0.3), starting from an X-ray selected sample, in the following way. For each object with $z \leq 0.3$, for each X-ray limiting sensitivity and for the adopted limiting magnitude $m_{B_{\rm lim}}$, we have computed the maximum redshift $z_{\rm max}$ at which the source would still be in the sample. There are thus two maximum redshift values to be calculated: the maximum z at which the source can be detected with a flux greater than or equal to the X-ray limiting sensitivity and the maximum z at which the source can be detected with a magnitude brighter than or equal to the adopted limiting magnitude $m_{B_{\rm lim}}$. The *minimum* of these two values is $z_{\rm max}$. This value of $z_{\rm max}$, combined with the solid angle of sky searched at that given X-ray limiting sensitivity, defines the volume available.[8] The fraction of this volume contained within $z = 0.3$ is retained, and all the

[8] The sky coverage used in this paper is reported in Table 2 of Maccacaro et al. (1991).

volumes are summed up to obtain the total volume searched, V_{S_i}. The contribution of each object i to the luminosity function is given by $1/V_{S_i}$. The integral optical luminosity function is then obtained by summing, in order of increasing absolute magnitude, the individual values of $1/V_{S_i}$, i.e.

$$N(<M_B) = \sum_{i:M_{B_i}<B} 1/V_{S_i} ,$$

over all the i objects with absolute magnitude brighter than M_B.

In order to obtain the differential optical luminosity function, we bin the individual contributions in bins of 1 mag. For each bin we have

$$dN(M_B)/dM_B = \sum_{i=1}^{N} 1/V_{S_i} ,$$

where N is the number of objects in the bin under consideration. The corresponding 68% error bars have been determined using the formula

$$\sigma_{\pm} = \left(\sum_{i=1}^{N} V_{Si}^{-2} \right)^{1/2} ,$$

which weighs each object by its contribution to the sum (see Marshall 1985 for details).

It is worth noting that, since we are using an X-ray selected sample of BLAGNs, the resulting optical spatial density would be a lower limit to the real spatial density of BLAGNs if a significant fraction of the BLAGNs population were X-ray-quiet. However, Avni & Tananbaum (1986), studying the X-ray properties of a sample of optically selected AGNs, have found that this is not the case and that no more than a few percent of AGNs can be X-ray-quiet.

The resulting local optical luminosity function is presented in Table 2 and is shown in Figure 3 (*filled circles*). We have verified, a posteriori, that the results are essentially unchanged by using a limiting magnitude, $m_{B_{\rm lim}}$, less than 20. In a similar way we have also verified that cosmological evolution effects are not important inside the chosen redshift range (0.0–0.3); a similar spatial density of BLAGNs, although with larger uncertainty, is obtained at each absolute magnitude if we restrict the analysis to the 75 objects with redshift less than 0.1. This is in agreement with the fact that the average V_e/V_a for $z \leq 0.3$ is 0.50 ($1\ \sigma = 0.02$), consistent with no evolution (see also Della Ceca et al. 1992 for a similar result on X-ray data only). Finally, we have also checked if the inclusion in the BLAGNs sample of the eight objects with poor S/N spectra (see § 2) could have a significant effect on the derived spatial density. One of these sources falls in the magnitude bin centered at -20, two sources fall in the magnitude bin centered at -21, and the remaining five sources fall in the magnitude bin centered at -22. Given the total number of objects in these three bins (13, 50, and 98 objects, respectively; see Table 2), the contribution of these eight sources to the total spatial density is less than 10% in each magnitude bin; i.e., their inclusion in the BLAGNs sample does not affect in any manner the derived spatial densities, and this also holds if all these eight objects should be of the narrow-line type.

TABLE 2

LOCAL OPTICAL LUMINOSITY FUNCTION

M_B	$N + 1\ \sigma$ ($Mpc^{-3}\ \Delta mag^{-1}$)	Objects
-19.....	$(2.91 \pm 1.57) \times 10^{-6}$	5
-20.....	$(2.25 \pm 0.74) \times 10^{-6}$	13
-21.....	$(3.47 \pm 0.74) \times 10^{-6}$	50
-22.....	$(2.83 \pm 0.65) \times 10^{-6}$	98
-23.....	$(5.61 \pm 2.75) \times 10^{-7}$	37
-24.....	$(1.03 \pm 0.23) \times 10^{-7}$	22
-25.....	$(4.26 \pm 4.26) \times 10^{-9}$	1

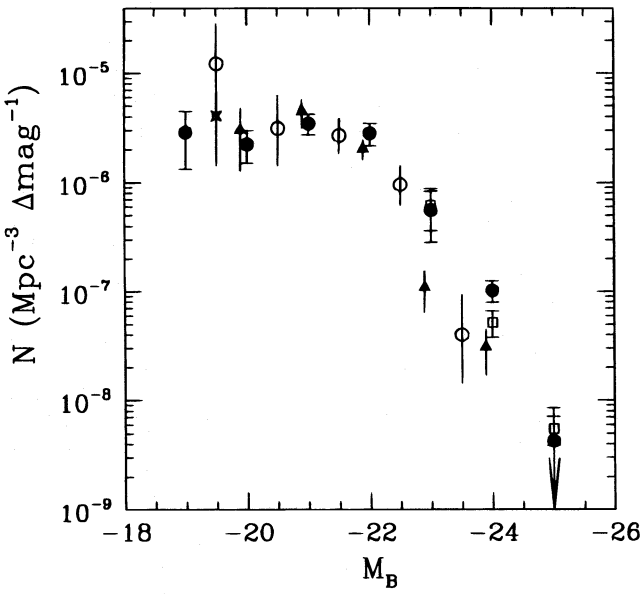

FIG. 3.—Local optical luminosity function of X-ray selected BLAGNs (*filled circles*). The open circles represent the local optical luminosity function of Seyfert 1 galaxies from the CfA sample (HB92). The star represents the density of the lowest luminosity bin of the optical luminosity function of Seyfert 1 galaxies from the CfA sample (HB92) corrected for the local density excess. The filled triangles represent the local optical luminosity function obtained from the Markarian survey of galaxies (MW84). The open squares at $M_B = -23$, -24, and -25 represent the density of "pointlike" BLAGNs with $z \leq 0.3$ as determined by Marshall (1985) using the BQS sample. (see § 3 for details).

It is now interesting to compare our results with the measured optical luminosity functions obtained from optical samples of BLAGNs (HB92 and MW84).

HB92 use the 26 Seyfert 1 galaxies present in the CfA redshift survey to compute the optical luminosity function. We have adjusted it to $H_0 = 50$ km s^{-1} Mpc^{-1} and $q_0 = 0$ and plotted it (*open circles*) in Figure 3.

MW84 use a sample of Seyfert galaxies selected from the first nine lists of the Markarian survey of objects with ultraviolet excess (Markarian & Lipovetskii 1976, and references therein). To avoid large correction factors for the incompleteness of the Markarian survey, these authors restricted the analysis to the sample of 51 Seyfert 1 galaxies with photographic magnitudes less than 15.5 and $z \leq 0.1$. After correcting for incompleteness at both bright and faint apparent magnitudes, they obtained the luminosity function reported in Figure 3 (*filled triangles*). The transformation $m_B = m_p + 0.11$ introduced by MW84 has been used to convert their blue photographic magnitudes into our magnitudes scale.

The overall shapes of all the luminosity functions are in good agreement with each other, although with some differences at both the low and the high-luminosity extremes. In particular our data points, which have on average smaller errors because of the better statistics (226 objects), lie lower

than HB92 at $M_B \sim -19.5$ and higher than the HB92 and MW84 data points at $M_B \leq -23$.

The higher density found by HB92 at $M_B \sim -19.5$ is probably due to local large-scale inhomogeneities in the galaxy density distribution (i.e., the Local super-cluster). As expressly cited in HB92 this effect may lead to an overestimate in the space density of the lowest luminosity objects when $1/V_a$ is used to estimate the luminosity function. We have checked this point by applying a density-independent method (STY method; Sandage, Tamman, & Yahil 1979) to the data of HB92. This maximum-likelihood method allows to determine the shape of the luminosity function, but not the normalization which should be derived using other statistical estimators. If we describe the liminosity function in the same way as HB92 (Schechter function; $\phi(M)dM \propto 10^{-0.4(M-M^*)(\alpha+1)} e^{-10^{-0.4(M-M^*)}} dM$; Schechter 1976) we find that the best-fit value for the power-law slope at low luminosity is $\alpha = -0.37 \pm 0.60$ (for the best-fit $M^* = -20.85$). This value must be compared with the value of -1.54 ± 0.30 (for the best-fit $M^* = -22.07$; $H_0 = 50$ km s^{-1} Mpc^{-1}) obtained from the fit of the luminosity function derived with $1/V_a$ method (see also HB92). This comparison confirms the suggestion of HB92 that the point at $M_B \sim -19.5$ may have been overestimated. To obtain a "correct" estimate for the density at $M_B \sim -19.5$ we have then used the following procedure. We have normalized the luminosity function obtained with the STY method with that given in HB92 at brighter absolute magnitude, where the effect of the Local supercluster is less important. The comparison of the spatial density of the two luminosity functions at $M_B \sim -19.5$ can be then used to estimate the overdensity in the HB92 derivation. Following this procedure we find a density excess of a factor ~ 3 in the lowest luminosity bin of the HB92 luminosity function. The density of the lowest luminosity bin of the HB92 luminosity function, corrected for this excess, is reported in Figure 3 (*the star*). From Figure 3 we notice that, after this correction has been taken into account, the three derivations of the optical luminosity function are in agreement with each other for faint magnitudes and all suggest a flattening at $M_B > -22$ as initially reported by MW84. Since this feature is clearly seen also in our X-ray selected sample, we are confident that this is an intrinsic property of the BLAGNs population rather than being due to incompleteness of the optically selected samples.

On the high-luminosity side ($M_B < -22.5$) we do not find evidence of the very strong decrease of the spatial density of broad-line AGNs which was suggested by the HB92 and MW84 luminosity functions. In particular, we find that the density of BLAGNs is about 3–6 times higher than that found by the CfA redshift survey and by the Markarian survey in the magnitude ranges centered at -23 and -24. This deficiency of objects may be due to selection effects of these two optical surveys. In the case of the CfA sample, at these luminosities, the optical selection criteria used to select local samples of active galaxies (i.e., spectroscopic investigation of a sample of galaxies) may fail in detecting them because objects with such bright nuclei may appear stellar and might not be included in the original list of galaxies to be investigated for activity. This point can be easily tested by using results from the Bright Quasar Survey (BQS; Schmidt & Green 1983). The objects that fail the criterion to be included in any galaxy lists but which also have a UV excess should show up in the BQS since it was selected specifically for "pointlike" sources. We have reported in Figure 3 (*open squares*) the density of BLAGNs with $z \leq 0.3$ in the magnitude range centered at -23, -24, and -25 as determined by Marshall (1985) using the BQS sample. As can be seen in Figure 3 the agreement between our spatial density and the spatial density determined by Marshall (1985) is very good. The only discordant point is that at $M_B = -24$, where we find a spatial density about a factor 2 higher than that obtained using the BQS sample. A similar incompleteness factor has been estimated by Markarian et al. (1987) by comparing the bright QSOs (satisfying the criteria $m_{pg} \leq 16$, $z \leq 0.16$, $M_{pg} \leq -23$, and $U-B < -0.44$) found in the BQS sample and in the Byurakan Sky Surveys. However, if the density of objects derived from HB92 (or from MW84) is added to the spatial density determined by Marshall (1985) (which could not be completely appropriate since there may be some overlap in the two samples), then the total spatial density derived from optical samples is consistent within 1 σ with the spatial density we have obtained using the EMSS X-ray selected sample of BLAGNs.

In conclusion, Figure 3 shows that the overall optical luminosity function of BLAGNs derived from an X-ray selected sample is in good agreement with that which can be obtained from optically selected samples by using different selection criteria in different ranges of absolute magnitude. This clearly shows the advantage of using X-ray selected samples for which a single selection criterion appears to work efficiently over the entire magnitude range.

4. THE NUCLEAR LUMINOSITY FUNCTION OF BLAGNs

The magnitudes we have used in the previous section are integrated magnitudes. However, the relevant quantity for the comparison of the luminosity function of local AGNs with the luminosity function derived from more distant quasars is the nuclear magnitude.

Since we have no information on the optical nuclear magnitude distribution for our sample of objects, we can obtain an estimate of the *nuclear* luminosity function only in a statistical way. To do this we must first investigate the properties of the host galaxies of Seyfert 1 and 1.5 nuclei. Two papers (Granato et al. 1993; Kotilainen & Ward 1994) have recently addressed this problem. Granato et al. (1993) have used CCD observations in the *BVR* optical bands of a sample of 42 optically selected Seyfert 1 and 1.5 galaxies to separate the galactic and nuclear fluxes. The studied objects were extracted from a homogeneous sample of 56 Seyfert 1 and 1.5 galaxies found in the area covered by the first nine Markarian lists (see Cheng et al. 1985 for the definition of this homogeneous sample). This sample of 56 objects was used by Cheng et al. (1985) to derive the nuclear luminosity function of Seyfert 1 and 1.5 nuclei. Kotilainen & Ward (1994) have used optical and infrared data on a hard X-ray selected sample of AGNs to investigate in detail the properties of the host galaxies.

To estimate how much the host galaxy luminosity contributes to the total luminosity, we have selected from the above mentioned papers all the Seyfert 1 and 1.5 galaxies (42 objects in total; see Table 3) for which galactic and nuclear *B* magnitudes are available. In Figure 4*a* we show the host galaxy luminosity versus the nuclear luminosity for this combined sample of Low Luminosity AGNs. As can be seen in this figure, there is a clear correlation between the nuclear and the host galaxy luminosity and, as pointed out,

TABLE 3

SEYFERT 1 AND 1.5 GALAXIES IN GRANATO ET AL. 1993 AND KOTILAINEN AND WARD 1994

Galaxy	Reference
0048+29	G
III Zw 2	K
3A 0557	K
ESO 198	K
H1847	K
Mrk 6	G
Mrk 79	G
Mrk 231	G
Mrk 290	G
Mrk 359	G
Mrk 506	G
Mrk 530	G
Mrk 590	GK
Mrk 668	G
Mrk 871	G
Mrk 1152	K
NGC 3227	K
NGC 3783	K
NGC 4593	K
NGC 5940	G
NGC 7469	GK
2237+07	G
3C 120	K
ESO 141	K
Fairall 9	K
IC 4329A	K
Mrk 10	G
Mrk 141	G
Mrk 279	G
Mrk 352	G
Mrk 372	G
Mrk 509	K
Mrk 584	G
Mrk 618	G
Mrk 704	G
Mrk 975	G
NGC 526a	K
NGC 3516	G
NGC 4151	K
NGC 5548	GK
NGC 7213	K
MCG −2-58-22	K

NOTE:—
G: from Granato et al., 1993; K: from Kotilainen et al., 1994; GK: objects in common between the two samples. For these objects we have taken a mean value for the galactic and nuclear magnitudes.

e.g., by Kruper & Canizares (1989) and by Kotilainen & Ward (1994), the more powerful AGNs reside in the more luminous host galaxies.

However, the distribution of the ratio between the nuclear and total luminosity is not constant over the entire range of total (i.e., nucleus + host galaxy) absolute magnitudes. This is seen in Figure 4*b* where we show M_B(Total) $- M_B$(Nuclear) $\equiv \Delta$ as a function of the total luminosity. This figure shows that the distribution of Δ is very broad with no evidence for a correlation between Δ and the total luminosity for M_B(Total) ≥ -22.6, while it becomes substantially narrower for $-22.6 \geq M_B$(Total) ≥ -24.0.

It is important to note that the optical and hard X-ray selected AGNs, shown in Figures 4*a* and 4*b*, have a very similar distribution of Δ values and according to a K-S test the two distributions are fully consistent with being extracted from the same parent population. This good agreement makes us more confident about using these data for our sample of soft X-ray selected AGNs.

On the basis of these data, we have derived the nuclear luminosity function using the following procedure.

The spatial density ($=1/V_{S_i}$) of each source i with total absolute magnitude equals to M_{B_i}(Total) has been split into j, M_{B_j}(Nuclear), bins of 1 magnitude, according to the probability, given by the normalized distribution of Δ, that the nuclear M_{B_i}(Nuclear) is in the bin j. All the contributions of the i different objects in the bin j are summed up to obtain the spatial density relative to the bin j at M_{B_j}(Nuclear).

The used normalized distribution of Δ is a uniform distribution in the range $-3 \leq \Delta \leq -0.5$ for M_B(Total) ≥ -22.6 and a uniform distribution in the range $-1.2 \leq \Delta \leq -0.5$ for M_B(Total) ≤ -22.6. Figure 4*b* shows that these limits on Δ enclose all the available data points with just two exceptions (NGC 7213, Mrk 668).

The resulting nuclear luminosity function is presented in Table 4 and is shown in Figure 5 (*filled circles*). The errors bars in the nuclear luminosity function have been obtained by adding, in quadrature, the 68% statistical errors associated with the number of objects expected in the bin j with an estimate of the errors associated with the Δ distribution. The latter has been obtained considering that we have about 10 objects for each bin of 1 magnitude around M_B(Total) ~ -21, -22, -23 (see Fig. 4*b*), which implies a relative error of about 30% on the derived spatial densities.

We advise the reader that a possible systematic error in our procedure could derive from the exclusion in this procedure of the tail of the Δ distribution which could reach, in principle, very small values. From the data reported in Figure 4*b* we have evidence of a cutoff of the Δ distribution at -3 for M_B(Total) ≥ -22.6 and -1.2 for M_B(Total) ≤ -22.6. A similar cutoff in the Δ distribution, although at a slightly lower value, is visible in Figure 6 of Kruper & Canizares (1989), who report galaxy and nuclear magnitudes for a sample of 43 soft X-ray selected AGNs. All but four of their objects have Δ less than ~ 1.5; the remaining four objects have only upper limits for Δ which could, in principle, be consistent with our chosen cutoffs. Therefore, from these data we have no compelling evidence of a significant fraction of BLAGNs objects with very small Δ values, but more data are needed to confirm this behavior. On the other hand, it is worth noting that the spatial density at M_B(Nuclear) ~ -17 would almost double if only 10% of the objects with M_B(Total) ~ -21 or -22 (where we see the flattening of the total luminosity function and we reach the maximum spatial density, see Fig. 3) have $\Delta = -5$ to

TABLE 4

NUCLEAR LUMINOSITY FUNCTION

M_B	$N \pm 1\,\sigma$ (Mpc^{-3} Δmag^{-1})
−16	$(6.67 \pm 6.14) \times 10^{-7}$
−17	$(1.49 \pm 0.88) \times 10^{-6}$
−18	$(2.45 \pm 0.96) \times 10^{-6}$
−19	$(3.16 \pm 1.06) \times 10^{-6}$
−20	$(2.50 \pm 0.82) \times 10^{-6}$
−21	$(1.14 \pm 0.39) \times 10^{-6}$
−22	$(5.82 \pm 2.01) \times 10^{-7}$
−23	$(1.20 \pm 0.43) \times 10^{-7}$
−24	$(1.17 \pm 0.85) \times 10^{-8}$

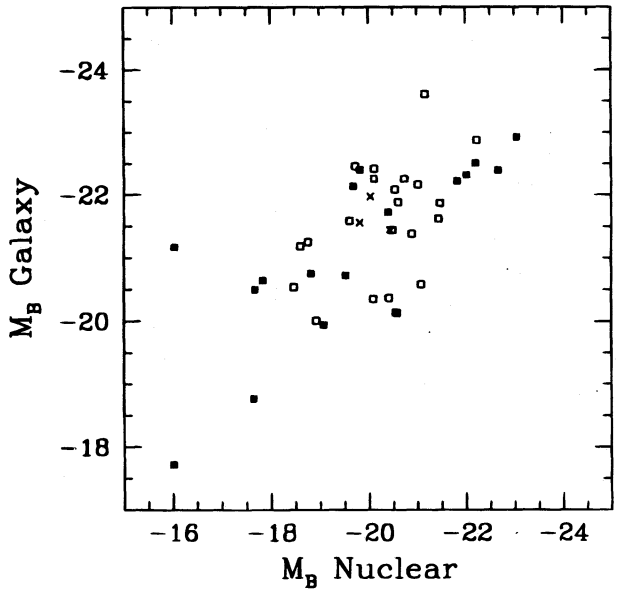

FIG. 4a

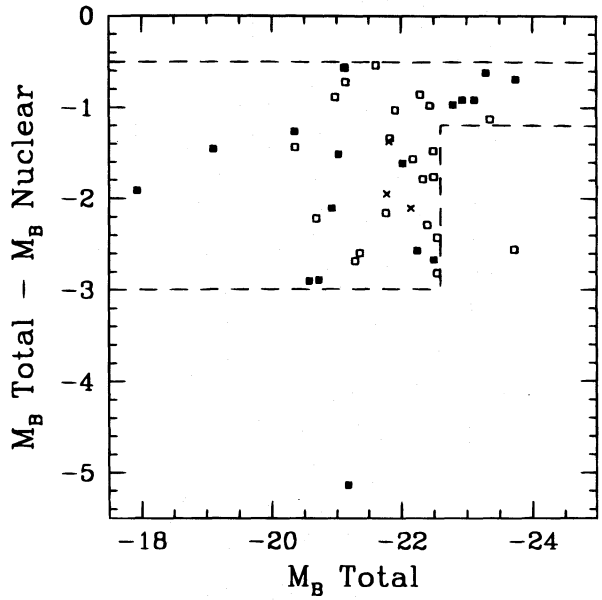

FIG. 4b

FIG. 4.—(*a*) Host galaxy absolute *B* magnitude vs. nuclear absolute *B* magnitude for the sample of Seyfert 1 and 1.5 galaxies with *B* magnitudes in the Granato et al. (1993) paper (*open points*) and in the Kotilainen & Ward (1994) paper (*filled points*). The crosses represent the three objects in common between the two samples. See Table 3. (*b*) M_B(Total) − M_B(Nuclear) ≡ Δ vs. M_B(Total) for the sample of Seyfert 1 and 1.5 galaxies with *B* magnitudes in the Granato et al. (1993) paper and in the Kotilainen & Ward (1994) paper. Symbols are the same as in Fig. 4*a*.

−4. On the basis of these considerations we warn the reader that the derived spatial density for M_B(Nuclear) ≥ −18 could be somewhat underestimated.

In Figure 5 we also report the nuclear luminosity function derived by Cheng et al. 1985 (*open circles*) and Marshall 1987 (*dotted line*) using optically selected samples of AGNs. As can be seen in this figure the overall agreement between our results and those obtained by Cheng et al. (1985) and M87 is quite good, although single data points may differ by as much as a factor of 2.

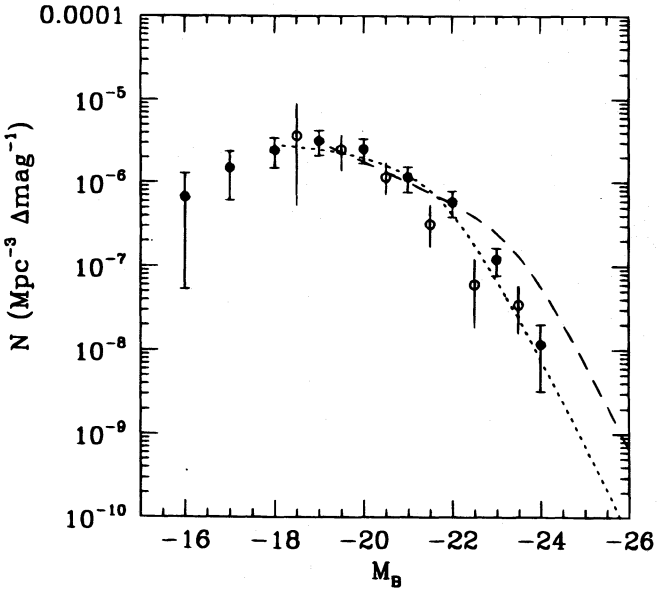

FIG. 5.—The filled circles represent the nuclear luminosity function obtained using the sample of X-ray selected BLAGNs in the EMSS. The open circles represent the nuclear luminosity function from Cheng et al. (1985) and the dotted line the nuclear luminosity function from Marshall (1987). The dashed line represents the expected spatial density of QSOs from La Franca et al. (1994), at $z = 0.15$. See § 4 for details.

In the same figure we also show the quasar luminosity function (*dashed line*) derived by La Franca et al. (1995) in the framework of a pure luminosity evolution model from a sample of more than 1000 optically selected quasars with $z < 2.2$ and $M_B < -23$. The quasar luminosity function has been de-evolved at low redshifts and plotted in Figure 5 for $z = 0.15$, the average redshift of our sample. Given the uncertainties in both our derivation of the nuclear luminosity function and the extrapolation of the quasar luminosity function, we conclude that the two luminosity functions are in rather good agreement, thus suggesting a continuity between local AGNs and more distant quasars.

5. THE OPTICAL LOG $N(<m_B) - m_B$ RELATIONSHIP OF BROAD LINE LOW LUMINOSITY ($M_B \geq -23$) AGN

In recent years the increased number (more than ∼1000 objects) of optically selected high-luminosity ($M_B \leq -23$) AGNs in *complete* samples has provided a good knowledge of their log $N(<m_B) - m_B$ relationship up to $m_B \sim 22.5$ (see e.g., the review of Hartwick & Shade 1990; Zamorani et al. 1991; Boyle et al. 1991b; Zitelli et al. 1992; La Franca et al. 1994; Trevese et al. 1994). On the other hand, the number of low-luminosity ($M_B \geq -23$) AGNs in complete sample is still very low (∼100 objects) and, as a consequence, their number-flux relationship is not well defined.

Having determined an estimate of the nuclear luminosity function of low-luminosity BLAGNs, we can now compute the log $N(<m_B) - m_B$ relationship for the objects with M_B(Nuclear) ≥ −23. This nuclear log $N(<m_B) - m_B$ relationship is shown in Figure 6 for two different cases: no evolution (*dotted line*) and evolution similar to that seen in QSOs samples [*dashed line*; $L^*(z) \propto (1+z)^{3.5}$ for $z \leq 2$ and $L^*(z) = L^*(z=2)$ for $z \geq 2$. See, e.g., La Franca et al. 1994]. The results shown in Figure 6 have been obtained by integrating the nuclear luminosity function (reported in Table

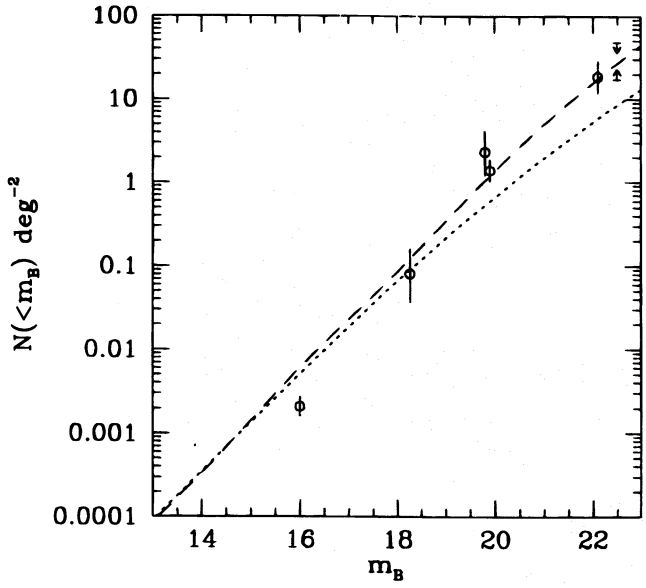

FIG. 6.—The predicted log $N(<m_B) - m_B$ relationship for the objects with M_B(Nuclear) ≥ -23 in the case of no-evolution (*dotted line*) and for a cosmological evolution similar to that of QSOs (*dashed line*). The open circles represent the spatial density of low-luminosity BLAGNs from different surveys. The downward and upward arrows represent the limits on the density of low-luminosity AGNs obtained using the sample of Trevese et al. (1994). See § 5 for details.

4) between $M_B = -15$ and $M_B = -23$ and up to redshift ~ 4. Note that this prediction refers to objects with *observed* M_B(Nuclear) greater than -23.

Also shown in Figure 6 is the optical spatial density of low-luminosity BLAGNs from different surveys (*circles*). The surface density at $m_B \sim 16$ has been determined using the 17 objects with $M_B \geq -23$ in the BQS sample. The completeness of the Seyfert subsample in the BQS has been largely discussed in the literature. We are aware that because of the stellar selection criterion adopted by Schmidt & Green such a sample is not intended to be complete in this range of magnitudes. From Figure 6 we can estimate a factor 3 of incompleteness of the Seyfert subsample in the BQS.

The surface density at $m_B \sim 18.3$, $m_B \sim 19.80$, $m_B \sim 19.9$, and $m_B \sim 22.1$ have been obtained using the three, four, 14, and seven objects with $M_B \geq -23$ in the BFG sample (Braccesi et al. 1980), in the BF sample (Marshall et al. 1984), in the SA 94 QSOs sample (La Franca et al. 1992), and in the MZZ sample (Zitelli et al., 1992; for this sample we have assumed $m_B = m_J + 0.1$), respectively. Finally the upper (*downward arrow*) and lower (*upward arrow*) limits at $m_B = 22.5$ have been obtained using the sample of variability selected objects in the 0.29 deg^{-2} area of SA 57 (Trevese et al. 1994). The lower limit has been obtained using only the five spectroscopically confirmed low-luminosity ($M_B \geq -23$) AGNs, while the upper limit has been obtained under the conservative hypothesis that the nine still unidentified objects with $m_B < 22.5$ (we have assumed $m_B = m_J + 0.1$) are low-luminosity AGNs. It is worth noting that in computing the optical surface densities of low-luminosity AGNs from optical surveys we have not used data from the Boyle et al. surveys (Boyle et al. 1990; Boyle, Jones & Shanks 1991a) because, as expressly reported in Boyle et al. (1991a), these surveys are not supposed to be complete for $z \leq 0.6$, i.e., where we expect the great majority of low-luminosity AGNs at the sampled apparent magnitudes.

As can be seen in this figure, the no-evolution case is inconsistent with the number density of low-luminosity BLAGNs found in these surveys. On the contrary, this figure clearly shows that the low-luminosity AGNs population has undergone, in the optical band, a cosmological evolution similar to that seen in the QSO samples (see also Setti 1984 and Zitelli et al. 1992 for a similar conclusion).

As can be deduced from Figure 5, the principal contribution to the log $N(<m_B) - m_B$ derives from objects with local nuclear luminosity in the range $M_B \sim [-18, -22]$. Since in this range of luminosity the nuclear luminosity function we have obtained is in good agreement with that derived using optical samples of low-luminosity BLAGNs, we are confident that the no-evolution case can safely be excluded. To quantify and describe in detail the evolution for these objects is a more difficult task. As discussed in § 3, using only the EMSS BLAGNs sample we have no indication of cosmological evolution within $z \leq 0.3$. As already noted by Marshall (1985) and Della Ceca et al. (1992), in this redshift domain the V_e/V_a method is rather insensitive to different evolution models and/or different values of the evolution parameter. Therefore, with the data at our disposal we cannot say if the low-luminosity BLAGNs follow, for example, a pure luminosity evolution model or a luminosity-dependent luminosity evolution model and/or at which z the evolution starts to be relevant.

6. SUMMARY AND CONCLUSIONS

In the recent past many authors have derived the local optical spatial density of BLAGNs, with some concerns about the completeness of the optically selected samples used.

To follow a different approach and to check the above-mentioned completeness problem we have used a complete sample of 226 local ($z \leq 0.3$) X-ray selected BLAGNs from the *Einstein Observatory* Extended Medium Sensitivity Survey. This sample represents the largest unbiased and complete sample of local BLAGNs ever assembled. Because of the large number of objects at our disposal, we have been able to set more stringent constraints on the space density of BLAGNs than previously possible.

The luminosity function derived from our sample is in good agreement with the composite luminosity function which can be derived from optically selected samples only by using different selection criteria in different ranges of absolute magnitude. In particular, at low luminosity ($M_B \geq -22$) we confirm the flattening of the local optical luminosity function originally suggested by Meurs & Wilson (1984), while in the magnitude range from $M_B \sim -23$ to -25 we find a very good agreement with the optical spatial density derived using data from the Bright Quasars Survey. The use of an X-ray selected sample has the advantage that a single selection criterion appears to work efficiently over the entire magnitude range.

By applying statistical corrections to the total magnitudes, we have also estimated the *nuclear* luminosity function of X-ray selected BLAGNs and compared it with the nuclear luminosity function obtained using optical selected samples of local AGNs. Good agreement between the two is found, although single data points may differ by as much as a factor of 2. Our nuclear luminosity function is also in good agreement with the extrapolation to low redshift of

the quasar luminosity function, thus suggesting a continuity between local AGNs and distant quasars.

Finally, by integrating this nuclear luminosity function over the $M_B - z$ plane, we find agreement with observed number counts of low-luminosity ($M_B \geq -23$) BLAGNs at faint magnitudes, if the $M_B \geq -23$ population evolves similarly to the QSOs population.

We would like to thank Isabella Gioia and Richard Griffiths for a careful reading of the manuscript and for useful comments. Suggestions from the anonymous referee have substantially improved this paper. This work has received partial financial support from the Italian Space Agency (ASI contracts 94-RS-41 191/3 AXG, 95-RS-152, 94-RS-96). R. D. C. acknowledges support from the NASA grant NAGW-3288. This research has made use of the NASA/IPAC Extragalactic Database (NED), which is operated by the Jet Propulsion Laboratory, Caltech, under contract with the National Aeronautics and Space Administration.

REFERENCES

Antonucci, R. 1993, ARA&A, 31, 473
Avni, Y., Bahcall, J. N. 1980, ApJ, 235, 694
Avni, Y., & Tananbaum, H. 1986, ApJ, 305, 83
Boyle, B. J., Fong, R., Shanks, T., & Peterson, B. A. 1990, MNRAS, 243, 1
Boyle, B. J., Jones, L. R., & Shanks, T. 1991a, MNRAS, 251, 482
Boyle, B. J., Jones, L. R., Shanks, T., Marano, B., Zitelli, V., & Zamorani, G. 1991b, in Proc. Workshop on Space Distribution of Quasars, ed. D. Crampton, (ASP Conf. Ser. 21), 1991
Braccesi, A., Zitelli, V., Bonoli, F., & Formiggini, L. 1980, A&A, 85, 80
Burstein, D., & Heiles, C. 1978, ApJ, 225, 40
Cavaliere, A., Giallongo, E., & Vagnetti, F. 1985, ApJ, 2996, 402
Cavaliere, A., & Padovani, P. 1988, ApJ, 333, L33
———. 1989, ApJ, 340, L5
Cheng, F. Z., Danese, L., De Zotti, G., & Franceschini, A. 1985, MNRAS, 212, 857
Comastri, A., Setti, G., Zamorani, G., & Hasinger, G. 1995, AA, 296, 1
Davis, M., Huchra, J., & Latham, D. 1983, in IAU Symp. 104, Early Evolution of the Universe and Its Present Structure, ed. G. Abell & G. Chincarini (Dordrecht: Reidel), 167
Della Ceca, R., Maccacaro, T., Gioia, I. M., Wolter, A., & Stocke, J. T. 1992, ApJ, 389, 491
Formiggini, L., Zitelli, V., Bonoli, F., & Braccesi, A. 1980, A&AS, 39, 129
Franceshimi, A., La Franca, F., Cristiani, S., & Martin-Mirones, J. M. 1994, MNRAS, 269, 683
Gioia, I. M., Maccacaro, T., Schild, R. E., Wolter, A., Stocke, J. T., Morris, S. L., & Henry, J. P. 1990, ApJ, 72, 567
Granato, G. L., Zitelli, V., Bonoli, F., Danese, L., Bonoli, C., & Delpino, F. 1993, ApJ, 89, 35
Griffiths, R. E., Della Ceca, R., Georgantopoulus, I., Boyle, B. J., Stewart, G. C., Shanks, T., & Fruscione, A. 1996, MNRAS, in press
Haehnelt, M. G., & Rees, M. J. 1993, MNRAS, 263, 168
Hartwick, F. D. A., & Shade, D. 1990, ARA&A, 28, 437
Ho, L. C., Filippenko, A. V., & Sargent, W. L. W. 1995, ApJS, 98, 477
Huchra, J., & Burg, R. 1992, ApJ, 90, 97 (HB92)
Huchra, J., Davis, L., Latham, D., & Tonry, J. 1983, ApJS, 52, 89
Kotilainen, J. K., & Ward, M. J. 1994, MNRAS, 266, 953
Kruper, J. S., & Canizares, C. R. 1989, ApJ, 343, 66
La Franca, F., Cristiani, S., & Barbieri, C. 1992, AJ, 103, 1062
La Franca, F., Gregorini, L., Cristiani, S., De Ruiter, H., & Owen, F. 1994, AJ, 108, 1548.
Maccacaro, T., Della Ceca, R., Gioia, I. M., Morris, S. L., Stocke, J. T., & Wolter, A. 1991, ApJ, 374, 117
Maccacaro, T., Gioia, I. M., Wolter, A., Zamorani, G., & Stocke, J. T. 1988, ApJ, 326, 680
Maccacaro, T., Wolter, A., McLean, B., Gioia, I. M., Stocke, J. T., Della Ceca, R., Burg, R., & Faccini, R. 1994, Astrophys. Lett. Comm., 29, 267
Madau, P. 1992, ApJ, 389, L1
Madau, P., Ghisellini, G., & Fabian, A. C. 1994, MNRAS, 270, L17
Markarian, B. E., Erastova, L. K., Lipovetskii, V. A., Stepanyan, Dzh, A., & Shapovalova, A. I. 1987, Astrofizika, 26, 7
Markarian, B. E., & Lipovetskii, V. A. 1976, Astrofizika, 12, 657
Marshall, H. L., Avni, Y., Braccesi, A., Huchra, J. P., Tananbaum, H., Zamorani, G., & Zitelli, V. 1984, ApJ, 283, 50
Marshall, H. L. 1985, AJ, 299, 109
———. 1987, AJ, 94, 628 (M87)
Meurs, E. J., & Wilson, A. S., 1984, A&A, 136, 206 (MW84)
Sandage, A., Tammann, G. A., & Yahil, A. 1979, ApJ, 232, 352
Schechter, P. 1976, ApJ, 203, 297
Schmidt, M. 1968, ApJ, 151, 393
Schmidt, M., & Green, R. F. 1983, ApJ, 269, 352
Setti, G. 1984 in X-Ray and UV Emission from Active Galactic Nuclei, ed. W. Brinkmann, J. Truemper, (MPE Rep. 184) 243
Stocke, J. T., Morris, S. L., Gioia, I. M., Maccacaro, T., Schild, R., Wolter, A., Fleming, T. A., & Henry, J. P. 1991, ApJS, 76, 813
Trevese, D., Kron, R. G., Majewski, S. R., Bershady, M. R., & Koo, D. C. 1994, ApJ, 433 494
Wilkes, J. B., Tananbaum, H., Worral, D. M., Avni, Y., Oey, M. S., & Flanagan, J. 1994, ApJS, 92, 53
Zamorani, G., Marano, B., Zitelli, V., Mignoli, M., Cimatti, A., & Boyle, B. J. 1991, in Proc. Workshop on Space Distribution of Quasars, ed. D. Crampton (ASP Conf.Ser. 21) 46
Zitelli, V., Mignoli, M., Zamorani, G., Marano, B., & Boyle, B. J. 1992, MNRAS, 256, 349